TB, PNM, PMB/209790, 30/01/2006

INSTITUTE OF PHYSICS PUBLISHING PHYSICS IN MEDICINE AND BIOLOGY

Phys. Med. Biol. **51** (2006) 1–10 doi:10.1088/0031-9155/51/0/000

Spatiotemporal signal space separation method for rejecting nearby interference in MEG measurements

S Taulu and J Simola

Elekta Neuromag Oy, Helsinki, Finland

E-mail: Samu.Taulu@neuromag.fi

Received 4 October 2005, in final form 28 November 2005
Published DD MMM 2006
Online at stacks.iop.org/PMB/51/1

Abstract

Counter-indications of traditional magnetoencephalography (MEG) exclude some important patient groups from MEG examinations, such as epilepsy patients with a vagus nerve stimulator, patients with magnetic particles on the head or having magnetic dental materials that cause severe movement-related artefact signals. Conventional interference rejection methods are not able to remove the artefacts originating this close to the MEG sensor array. For example, the reference array method is unable to suppress interference generated by sources closer to the sensors than the reference array, about 20–40 cm. The spatiotemporal signal space separation method proposed in this paper recognizes and removes both external interference and the artefacts produced by these nearby sources, even on the scalp. First, the basic separation into brain-related and external interference signals is accomplished with signal space separation based on sensor geometry and Maxwell's equations only. After this, the artefacts from nearby sources are extracted by a simple statistical analysis in the time domain, and projected out. Practical examples with artificial current dipoles and interference sources as well as data from real patients demonstrate that the method removes the artefacts without altering the field patterns of the brain signals.

(Some figures in this article are in colour only in the electronic version)

1. Introduction

Biomagnetic measurements offer invaluable information for both basic research and clinical neurology. For example, magnetoencephalography (MEG) noninvasively maps the magnetic sources in the brain with good spatial and excellent temporal resolution (Hämäläinen *et al* 1993). MEG measurements are used for many patient groups, especially in presurgical mapping of patients with epilepsy or tumours.

Unfortunately, the MEG method is known to suffer from aggravating technical problems that have no counterpart for example in the EEG recording technique. One of them is strong

interference arising from sources of magnetic field in the environment or even on the body and head of the patient. The interference from the surrounding technical infrastructure and instrumentation is conventionally dealt with by installing the MEG device in a magnetically shielded room (MSR) with a high enough shielding factor to reduce the interference inside the room to a tolerable level. Consequently, in clinical environment the MSR will keep the recorded signals well within the dynamic range of the MEG device but software methods are still needed to further reduce the interference effects to low enough level on the biomagnetic scale. Several interference suppression methods have been developed for interference sources located far away from the sensors. These methods include e.g. gradiometric coil configurations (Zimmerman 1977), reference sensors (Vrba and Robinson 2001), signal space projection (SSP) (Uusitalo and Ilmoniemi 1997), and most recently the signal space separation (SSS) method (Taulu and Kajola 2005, Taulu *et al* 2005).

If the sources of magnetic interference are inside the MSR, the situation is more difficult to deal with by using reference sensors or standard SSP based on a statistical analysis of empty room data. Such sources may consist of instrumentation used for stimulation, EEG electrodes on the patient's head magnetized e.g. in a prior MRI recording, or metal parts or residue on the patient's body or scull as a result of medical operations. It has been shown (Taulu *et al* 2005) that with an accurately calibrated multichannel device, the SSS method provides shielding exceeding a factor of 150 even for sources as close as 1 m and a factor of 50 for sources at 0.5 m from the sensors. This already greatly exceeds the interference suppression achieved for such nearby sources by the conventional reference sensor method. In clinical work, however, significant artefact sources much closer than this exist.

In basic academic brain research, the problems with nearby sources may be avoided by using only dedicated stimulators that do not produce magnetic interference, by leaving out the EEG electrodes if they turn out to be magnetic and by avoiding use of subjects having magnetic components or residue in/on their body, dental work, braces etc. In clinical MEG work, however, standard clinically approved stimulus devices must be used, EEG may be compulsory for regulatory reasons, and also patients carrying magnetic impurities must be examined.

Especially, metal parts or residue on the body or scull of the patient usually cause a highly distorted MEG signal due to even minimal involuntary motion, and have been considered a counter-indication for MEG-based diagnostics. The method described in this paper aims at removing these constraints on the applicability of MEG in clinical work where this kind of interference sources are rather common and have to be dealt with.

2. Overview of interference rejection methods

2.1. The reference array method

The basic problem in all interference rejection is how to find out which part of the recorded signal is interference. When this is known, the rejection can be made by a simple subtraction or projection. The conventional way to recognize interference is to use a dedicated reference sensor array located so far away from the head of the subject that all the signals detected by the reference array can be assumed to be interference (Vrba and Robinson 2001).

The problem with this method is that the amount of signal to be subtracted from the proper signal channels as interference must be extrapolated across the distance from the reference array to the proper sensors, about 20–40 cm. For far away interference sources, causing relatively uniform fields, this extrapolation may succeed so well that interference rejection by a factor of 10 or even 100 is possible (Vrba and Robinson 2001). But for interference sources

inside the MSR located a few times the extrapolation distance, about 1 m, away from the sensor helmet, the interference rejection provided by the reference array method is considerably less. This is because the field produced by such sources is highly non-uniform and to extrapolate it accurately over the volume of the sensor helmet would require knowing derivatives of the field up to a high order. In principle, this would be possible if a very large number of reference channels, properly distributed and oriented, were available, but not with a realistic number of reference channels, 30 or so.

Furthermore, for interference sources closer to the helmet than the extrapolation distance, for example magnetic impurities on the head of the patient or magnetized EEG electrodes, the reference sensor method does not work at all, not even in principle. This is because the radius of convergence of any series expansion, e.g. Taylor's, used to extrapolate the interference field, is determined by the location of the interference source. If there are MEG channels that are closer to the reference channels than the interference source, and other MEG channels that are further away from the reference sensors than the interference source, then two different series expansions would be needed to correctly extrapolate the interference amplitudes seen in these two groups of channels. Additionally, when the source of interference, e.g. magnetic impurity on the scalp, is moving with the patient's head, which is required to produce the interference, we would not know exactly which channels belong to the two groups at a certain moment of time. Therefore, the extrapolation process based on a reference sensor system would be rather complicated to handle.

2.2. Reference sensor free interference rejection

In the SSS method, the interference signal to be subtracted is determined without using any dedicated reference sensors; all MEG channels record signals from both the brain and the interference sources. Because the interference is recorded by the same sensors as the brain signals, it is recorded at the very location where it needs to be known, and there is virtually no extrapolation distance associated with this method.

In SSS, the resolution between signal of interest and interference is based on the distribution of the signals over the entire sensor array. The method relies on accurate calibration of sensors and Maxwell's equations. In a properly designed sensor array, the SSS method does not increase sensor noise (Taulu *et al* 2005).

The SSS method described in Taulu and Kajola (2005) and Taulu *et al* (2005) is a purely spatial method. Each momentary signal vector is resolved into components arising from inside and into components arising from outside of the sensor helmet. As shown in Taulu *et al* (2005), such a purely spatial algorithm results in an interference rejection factor that grows continuously and monotonously with increasing distance of the interference source. To further sharpen the SSS resolution so that rejection of interference from sources even on the scalp of the patient becomes possible, we have developed an SSS-based statistical method that is the subject of this paper. Section 3 describes the statistical algorithm. Examples of application of the method on phantom experiments and real physiological data are presented in section 4.

3. Method

3.1. The spatial SSS method

Signal space separation is a purely spatial method to transform electromagnetic multichannel data into uncorrelated basic components, e.g. magnetic multipole moments (Taulu and Kajola 2005, Taulu *et al* 2005). With SSS, it is possible to uniquely estimate the multipoles separately for the signals arising from the internal and external volumes of the sensor array. Consequently,

in MEG the brain signals can be extracted from the measured data on the basis of the geometry of the sensor configuration. The method does not alter the field distribution of the biomagnetic signal. By calculating the multipoles as fixed to the coordinate system of the head, one gets a device-independent representation for the biomagnetic signals free of interference and distortions caused by changes in the head position with respect to the measurement device.

The SSS method relies on the fact that with a modern multichannel device, comprising up to more than 300 independent sensors, it is possible to estimate all degrees of freedom of the biomagnetic field that have high enough amplitude to exceed the noise levels of the sensors. SSS is based directly on Maxwell's equations and the assumption that the sensors are at least 2–4 cm away from all sources of magnetic field. In this model, the biomagnetic and external interference signals are expanded in terms of harmonic basis functions converging at infinity and at the origin, respectively. Consequently, the signal vector ϕ composed of the values from the N channels can be given in the matrix form:

$$\phi = \mathbf{S}\mathbf{x} = [\mathbf{S}_{\text{in}}\ \mathbf{S}_{\text{out}}] \begin{bmatrix} \mathbf{x}_{\text{in}} \\ \mathbf{x}_{\text{out}} \end{bmatrix}, \tag{1}$$

where the SSS basis $\mathbf{S}$, composed of elementary signal vectors corresponding to the harmonic basic functions, is divided into separate subspaces $\mathbf{S}_{\text{in}}$ and $\mathbf{S}_{\text{out}}$ related to the biomagnetic and external interference signals, respectively. The vector of multipole moments, $\mathbf{x}$, contains separate components for the biomagnetic and external interference sources. In other words, the elements of $\mathbf{x}$ are the weights of the different basis vectors of $\mathbf{S}$ corresponding to the given ϕ. In constructing the SSS basis, the two series of harmonic functions are truncated at orders L_{in} and L_{out}, giving dimension

$$n = (L_{\text{in}} + 1)^2 + (L_{\text{out}} + 1)^2 - 2 \tag{2}$$

for the basis. Determination of proper values for L_{in} and L_{out} has been investigated in detail in Taulu and Kajola (2005) and Taulu *et al* (2005). In the case of MEG, the values $L_{\text{in}} = 8$ and $L_{\text{out}} = 3$ have been found sufficient leading to $n = 95$. With modern multichannel devices, $N > n$ and the SSS basis is thus linearly independent for practical sensor arrays allowing one to uniquely estimate the multipole moments from the signal vector ϕ:

$$\hat{\mathbf{x}} = \begin{bmatrix} \hat{\mathbf{x}}_{\text{in}} \\ \hat{\mathbf{x}}_{\text{out}} \end{bmatrix} = \mathbf{S}^{\dagger}\phi, \tag{3}$$

where $\mathbf{S}^{\dagger}$ is the pseudoinverse of $\mathbf{S}$. The accuracy of $\hat{\mathbf{x}}$ depends on both the condition number of $\mathbf{S}$ and the calibration accuracy of the device since the method is based on the accurate knowledge of the geometry of the sensor array.

Using these multipole moments, one can reconstruct the signals corresponding to the biomagnetic and external interference sources as

$$\hat{\phi}_{\text{in}} = \mathbf{S}_{\text{in}}\hat{\mathbf{x}}_{\text{in}}, \tag{4}$$

$$\hat{\phi}_{\text{out}} = \mathbf{S}_{\text{out}}\hat{\mathbf{x}}_{\text{out}}. \tag{5}$$

3.2. Limitations of SSS

The two mechanisms that determine the accuracy of the SSS reconstruction are truncation error related to the termination of the harmonic expansions and calibration inaccuracies of the MEG sensor array. The reconstruction errors are then

$$\hat{\mathbf{x}}_{\text{in},\epsilon} = \hat{\mathbf{x}}_{\text{in,t}} + \hat{\mathbf{x}}_{\text{in,c}}, \tag{6}$$

$$\hat{\mathbf{x}}_{\text{out},\epsilon} = \hat{\mathbf{x}}_{\text{out,t}} + \hat{\mathbf{x}}_{\text{out,c}}, \tag{7}$$

where t and c indicate truncation and calibration errors, respectively. In practice, with modern multichannel devices using thin-film sensor technology, a calibration accuracy of about 0.1% can be achieved in sensitivity, location, orientation, gradiometer balance and cross-talk between the channels (Taulu *et al* 2005). The remaining inaccuracy results in insignificantly small reconstruction errors, provided that there are no sources of magnetic field in the measurement volume (Taulu *et al* 2005).

However, for interference sources in the immediate vicinity of the sensors, the spatial SSS model with finite truncation orders leads to leakage of the interference contribution into both internal and external multipoles as the signals do not completely fall on $\mathbf{S}_{\text{in}}$ or $\mathbf{S}_{\text{out}}$, even with perfect calibration accuracy. The statistical method described below is based on this leakage phenomenon.

3.3. The spatiotemporal SSS method

Because SSS cannot separate sources very close to the sensors, we can recognize such sources by extracting temporal components that are common to $\hat{\mathbf{x}}_{\text{in}}$ and $\hat{\mathbf{x}}_{\text{out}}$. Then, the extracted components can be projected out from the SSS reconstructed signals. This does not affect the brain signals which are temporally uncorrelated with the external interference and artefacts arising from the intermediate space.

3.4. The algorithm

Consider now the data matrix $\Phi = [\phi(t_1) \cdots \phi(t_m)]$ containing m signal vectors measured at time instants $t_1, t_2, \ldots, t_m$. The corresponding SSS reconstruction results using (3) are

$$\hat{\mathbf{X}}_{\text{in}} = \hat{\mathbf{X}}_{\text{in},0} + \hat{\mathbf{X}}_{\text{in},\epsilon}, \tag{8}$$

$$\hat{\mathbf{X}}_{\text{out}} = \hat{\mathbf{X}}_{\text{out},0} + \hat{\mathbf{X}}_{\text{out},\epsilon}, \tag{9}$$

where the subscript 0 indicates undistorted reconstruction and ϵ signifies combined truncation and calibration error according to (6) and (7). Now matrices $\hat{\mathbf{X}}_{\text{in}}$ and $\hat{\mathbf{X}}_{\text{out}}$ have dimensions $n_{\text{in}} \times m$ and $n_{\text{out}} \times m$, respectively, with

$$n_{\text{in}} = (L_{\text{in}} + 1)^2 - 1, \tag{10}$$

$$n_{\text{out}} = (L_{\text{out}} + 1)^2 - 1. \tag{11}$$

Obviously, the undistorted estimates $\hat{\mathbf{X}}_{\text{in},0}$ and $\hat{\mathbf{X}}_{\text{out},0}$ are temporally uncorrelated as the former only contains the biomagnetic signals of interest and the latter has contribution from the external interferences only. In contrast, truncation and calibration errors cause mixing of the multipole moments and thus generate similar temporal patterns in $\hat{\mathbf{X}}_{\text{in},\epsilon}$ and $\hat{\mathbf{X}}_{\text{out},\epsilon}$. To model the problem, let $\mathbf{C}_{\text{in}}$ and $\mathbf{C}_{\text{out}}$ be the temporal domain bases spanning $\hat{\mathbf{X}}_{\text{in}}$ and $\hat{\mathbf{X}}_{\text{out}}$, respectively, and let $\mathbf{L} = \mathbf{C}_{\text{in}} \cap \mathbf{C}_{\text{out}}$ be the intersection of these bases which contains only those time domain signals that are common to $\hat{\mathbf{X}}_{\text{in},\epsilon}$ and $\hat{\mathbf{X}}_{\text{out},\epsilon}$. The bases $\mathbf{C}_{\text{in}}$ and $\mathbf{C}_{\text{out}}$ can be calculated e.g. by performing the singular value decomposition (SVD) on matrices $\hat{\mathbf{X}}_{\text{in}}$ and $\hat{\mathbf{X}}_{\text{out}}$. In the absence of nearby interference sources, $\mathbf{L}$ is empty if calibration is perfect. When nearby sources are present, the rank of $\mathbf{L}$ is the dimension of the artefact signal in the time domain describing the complexity of the interference signal to be removed. For the calculation of the intersection $\mathbf{L}$, see e.g. Golub and Van Loan (1996).

The time patterns contained in $\mathbf{L}$ can be removed e.g. by projecting the signals into the orthogonal complement of $\mathbf{L}$ in the time domain. When $\mathbf{L}$ is an orthonormal basis, then the

desired projection operator is $\mathbf{I} - \mathbf{L}\mathbf{L}^{\mathrm{T}}$, where $\mathbf{I}$ is the identity matrix and T means transpose. Thus, the projected components are given as

$$\hat{\mathbf{X}}_{\mathrm{in,p}} = \left[(\mathbf{I} - \mathbf{L}\mathbf{L}^{\mathrm{T}})\hat{\mathbf{X}}_{\mathrm{in}}^{\mathrm{T}}\right]^{\mathrm{T}}. \tag{12}$$

According to the previous arguments, the mixing of the multipoles is contained in $\mathbf{L}$ and thus $\left[(\mathbf{I} - \mathbf{L}\mathbf{L}^{\mathrm{T}})\hat{\mathbf{X}}_{\mathrm{in},\epsilon}^{\mathrm{T}}\right]^{\mathrm{T}} = \mathbf{0}$. Furthermore, any randomly chosen high-dimensional vectors are approximately orthogonal to each other and therefore the brain and interference signals are, across a long enough time, close to orthogonal leading to

$$\hat{\mathbf{X}}_{\mathrm{in,p}} \approx \hat{\mathbf{X}}_{\mathrm{in},0}. \tag{13}$$

The projection operation in (12) is called the signal space projection (SSP) which has been widely used in MEG in the spatial domain mainly to remove external interference (Uusitalo and Ilmoniemi 1997). The spatial SSP slightly changes the field pattern of the brain signals which has to be taken into account in source modelling. In our new method, SSP is performed in the time domain and thus the spatial pattern of the brain signals is not affected even if they are not orthogonal to the interference. No compensation of the projection operator (12) is needed in the source modelling.

The above algorithm has been described for the estimated multipole moments. However, instead of $\hat{\mathbf{X}}_{\mathrm{out}}$ one could also use $\hat{\Phi}_{\mathrm{out}}$ or $\hat{\Phi}_{\mathrm{residual}} = \Phi - (\hat{\Phi}_{\mathrm{in}} + \hat{\Phi}_{\mathrm{out}})$. Similarly, $\hat{\mathbf{X}}_{\mathrm{in}}$ could be replaced by $\hat{\Phi}_{\mathrm{in}}$ and $\mathbf{L}$ could be replaced with some other relevant basis spanning the interference time patterns.

In comparing the temporal domain bases $\mathbf{C}_{\mathrm{in}}$ and $\mathbf{C}_{\mathrm{out}}$, a small positive inaccuracy $\delta \ll 1$ must be allowed for so that two vectors are considered identical when the angle θ between them has $\cos\theta > 1 - \delta$. This is because real signals always include noise. If δ is chosen too small, one rejects the highest amplitude interference only. When increasing δ, a risk is taken to exclude some brain signals also. Because the interference signals typically have considerably higher amplitude than the biomagnetic signals, it is rather easy to determine δ so that all interference is removed and all biomagnetic signals retained. In the examples below, we have used $\delta = 0.01$–0.05.

4. Results

4.1. Phantom experiment

The performance of our SSS-based interference rejection was first tested by phantom experiments. The ability of the method to remove artefacts even from sources directly on the surface of the head was examined by simultaneous activation of the most superficial current dipole in a phantom and a small magnetic dipole on the outer surface of the phantom, just 16 mm above the current dipole. The current dipole was energized by two periods of a sine wave pulse and the magnetic dipole by a continuous sine wave at the same frequency. The unprocessed data contain contributions from both magnetic sources superimposed as seen in figure 1. Application of the spatiotemporal SSS completely removes the continuous sinusoidal signal from the magnetic dipole on the surface of the phantom, leaving the sine wave pulse from the current dipole intact. Note that the resolution between these two sources could not have been achieved by simple low-pass or high-pass filtering because the sources have the same frequency.

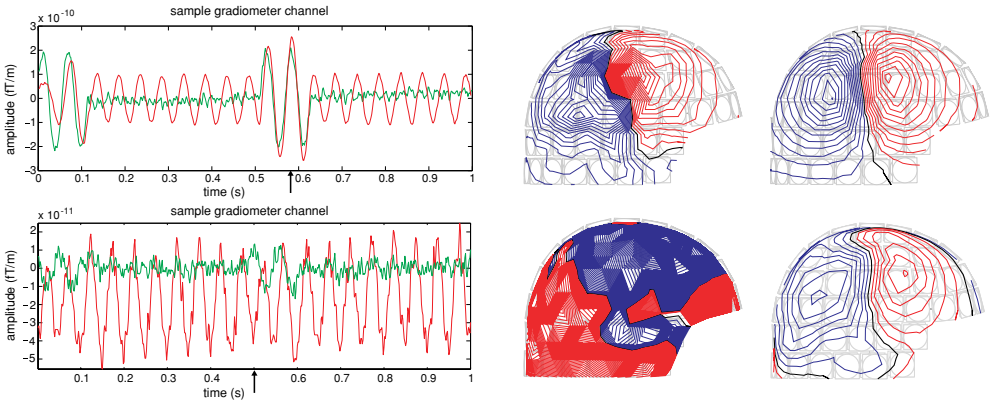

Figure 1. Unaveraged single epoch results from a phantom experiment with simultaneously activated superficial current dipole and a magnetic dipole attached to the surface of the phantom head directly above the dipole. Left column: original (red) and SSS reconstructed (green) waveforms from sample gradiometer channels when current dipole moments of 2000 nA m (top) and 50 nA m (bottom) were used. Middle column: the corresponding unprocessed field distributions at the peaks indicated by arrows. Right column: the corresponding SSS reconstructed fields. An SSS basis with $L_{\mathrm{in}} = 8$ and $L_{\mathrm{out}} = 3$ was used for the spatiotemporal SSS processing. Note that the amplitude scales on the first and second rows are different.

4.2. Software magnetic shielding

The previous example showed that the extended SSS is able to remove the artefact signals even from the closest possible interference sources while keeping the spatial distribution of the brain signals intact. The shielding factor provided by the method against artefacts is practically infinite because the accurate time pattern of the interference is suppressed by the projection operation defined by (12). In other words, the amplitude of the artefact is reduced down to the noise level and the actual shielding factor essentially equals the artefact-to-noise ratio.

To show this, we recorded data with a strong artefact source, a magnetic dipole, located in the middle of the opening of the helmet-shaped Elekta Neuromag whole head sensor array. The distance of this source from the centre of the device coordinate system was about 10 cm. As there were no sources inside the helmet, the successful reconstruction of the signals arising from the inner volume of the helmet should contain some sensor noise only. Figure 2 shows the reconstruction result. Clearly, the artefact signal is removed completely. This is obvious also from the field maps on the right-hand side of figure 2. To further verify that the artefact was really suppressed below the noise level on all channels of the sensor array, the following statistical analysis was made. In a high-dimensional space, any two randomly chosen vectors are approximately orthogonal to each other. Therefore, in the presence of random sensor noise, the quality of the reconstruction result can be examined by calculating the angle between the original and the reconstructed time domain signal. In the case of perfect artefact suppression, the reconstructed result has no correlation with the original signal and the expectation value of the angle is the same as that for randomly chosen vectors. In this example, the examined time span was 2 s, corresponding to 1200 samples. The mean of the aforementioned angle over all 306 channels was 89.1°. For comparison, 306 pairs of normally distributed 1200 dimensional random vectors were produced and the mean of the corresponding 306 angles was calculated. The result was 88.7° which is close enough to that calculated from the comparison of the original and the SSS results for one to conclude that the shielding factor of the method is practically infinite.

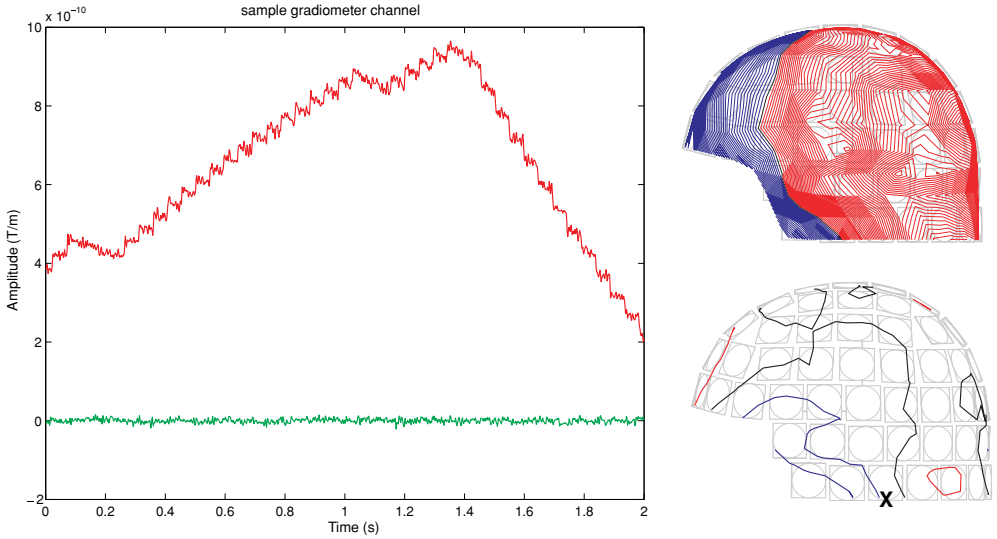

Figure 2. The artefact signal (red) produced by a source located in the immediate vicinity of the sensors and the corresponding SSS reconstructed result (green) from a sample gradiometer channel. The upper and lower field distributions correspond to original and SSS reconstructed data, respectively. The location of the artefact source is marked by x. The contour step is 200 fT.

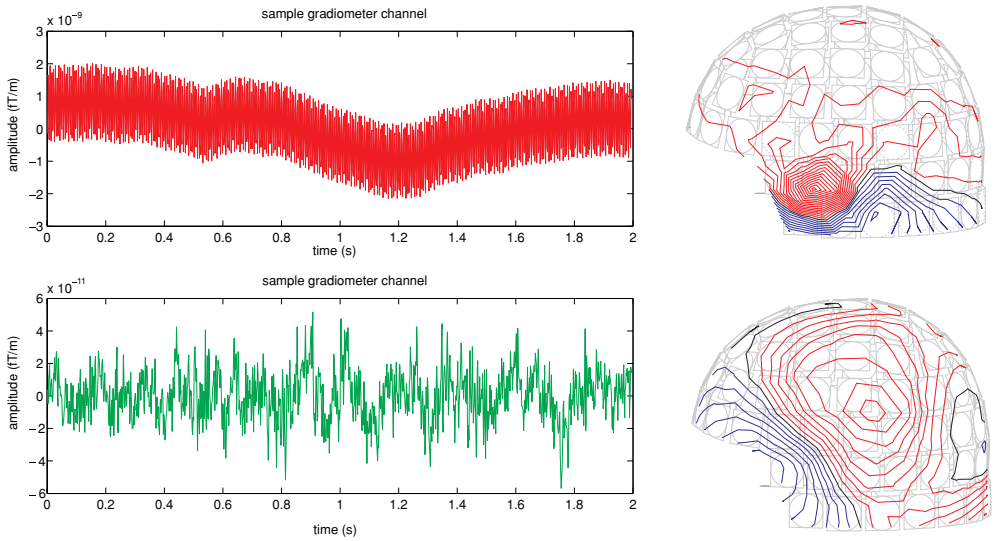

Figure 3. Signals from a patient with a VNS and continuously active head position indicator coils. Top: original sample waveform and field distribution at 1.3 s. Bottom: the same sample waveform SSS reconstructed and the corresponding field distribution showing a single auditory response. (Courtesy of Dr Ritva Paetau, Helsinki University Central Hospital.)

4.3. Examples of physiological measurements

Figure 3 shows a single evoked auditory response from a patient having a vagus nerve stimulator (VNS) and continuously activated head position indicator (HPI) coils. The original data are dominated by the large VNS artefact and high-frequency HPI signals, both of which are

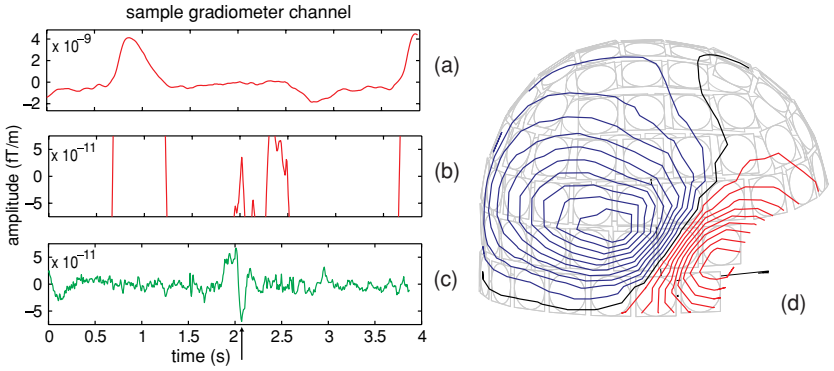

Figure 4. (a) A planar gradiometer tracing over the right frontal lobe. The signal range is 5×10^{-9} T m^{-1} before the SSS interference cancellation. (b) The same signal on a physiological scale, magnified by 50. (c) After suppressing the interference due to the VNS by spatiotemporal SSS, the channel shows an epileptic spike with the magnitude of about ± 500 fT cm^{-1}. (d) Isocontour field of the epileptic spike seen in (c) points to the source in the right frontal lobe. (Courtesy of Dr Michael Funke, University of Utah.)

removed by SSS leaving only the auditory field intact. The ability to clearly see the field pattern even of a single trial response in the reconstructed data demonstrates the efficacy of the interference suppression.

Another VNS case is illustrated in figure 4. During the MEG recording of spontaneous data, the VNS was not stimulating, but still created huge disturbances to the signals. After SSS reconstruction, epileptic spikes corresponding to a dipole in the right frontal lobe are easily identified.

5. Conclusions

The spatiotemporal signal space separation method described in this paper makes it possible to get meaningful clinical MEG recordings on patient groups having so far been excluded from biomagnetic measurements. Such subjects, having stimulators or other magnetic devices or residue in/on their body or head, are even more common among neurological patients than in the rest of the population.

The sources of magnetic interference associated with these subjects are either small residual magnetism on the scull or scalp, quite next to the MEG sensors, or larger magnetic objects further away in their body, but on the opposite side of the MEG sensor array than the reference sensor system. Therefore, no reference sensor arrangement enables efficient rejection of the resulting interference.

We have demonstrated a way for sharpening the spatial resolution of the signal space separation method by a statistical algorithm enabling us to overcome the basic limitations of conventional interference rejection methods and to expand the clinical utility of MEG.

Acknowledgments

The authors thank Dr Michael Funke and Dr Ritva Paetau for supplying us with patient data and for stimulating the development of the presented method. The authors also acknowledge Dr Antti Ahonen for invaluable comments and criticism on the manuscript.

References

Golub G H and Van Loan C F 1996 *Matrix Computations* 3rd edn (Baltimore, MD: Johns Hopkins University Press) **See endnote 1**

Hämäläinen M, Hari R, Ilmoniemi R, Knuutila J and Lounasmaa O 1993 Magnetoencephalography—theory, instrumentation, and applications to noninvasive studies of the working human brain *Rev. Mod. Phys.* **65** 413

Taulu S and Kajola M 2005 Presentation of electromagnetic multichannel data: the signal space separation method **See endnote 2** *J. Appl. Phys.* **97**

Taulu S, Simola J and Kajola M 2005 Applications of the signal space separation method *IEEE Trans. Signal Process.* **53** 3359

Uusitalo M and Ilmoniemi R 1997 Signal-space projection method for separating MEG or EEG into components *Med. Biol. Eng.* **32** 35

Vrba J and Robinson S 2001 Signal processing in magnetoencephalography *Methods* **25** 249

Zimmerman J 1977 SQUID instruments and shielding for low-level magnetic measurements *J. Appl. Phys.* **48** 702

Endnotes

(1) Author: Please check the initial(s) of the authors in reference 'Golub and Van Loan (1996)'.
(2) Author: Please provide the page number(s) in reference 'Taulu and Kajola (2005)'.
(3) Author: Please let us know if you are willing to pay a total of £570 for colour print reproduction of your four figures. If so, please let us know to whom and where (including the VAT number of the institution) we should send the invoice.
